

# CIMRL: Combining IMitation and Reinforcement Learning for Safe Autonomous Driving

Jonathan Booher   Khashayar Rohanimanesh   Junhong Xu   Vladislav Isenbaev\*

Ashwin Balakrishna\*   Ishan Gupta\*   Wei Liu\*   Aleksandr Petiushko

Nuro, Inc.

**Abstract:** Modern approaches to autonomous driving rely heavily on learned components trained with large amounts of human driving data via imitation learning. However, these methods require large amounts of expensive data collection and even then face challenges with safely handling long-tail scenarios and compounding errors over time. At the same time, pure Reinforcement Learning (RL) methods can fail to learn performant policies in sparse, constrained, and challenging-to-define reward settings like driving. Both of these challenges make deploying purely cloned policies in safety critical applications like autonomous vehicles challenging. In this paper we propose Combining IMitation and Reinforcement Learning (CIMRL) approach — a framework that enables training driving policies in simulation through leveraging imitative motion priors and safety constraints. CIMRL does not require extensive reward specification and improves on the closed loop behavior of pure cloning methods. By combining RL and imitation, we demonstrate that our method achieves state-of-the-art results in closed loop simulation driving benchmarks.

## 1 Introduction

The development of self-driving cars has been mainly driven by advancements in three key areas: perception, prediction, and planning. These components form the foundation of modern the self-driving car stack (SDC), enabling autonomous vehicles to navigate safely and efficiently. In recent years, deep learning has significantly transformed the design of SDC, particularly revolutionizing the first two components: perception [1, 2, 3], and prediction [4, 5, 6]. Most of these prior works leverage supervised learning on large, manually or auto-labeled datasets and curated expert driving behavior. Methods like behavior cloning (BC) and other imitation learning (IL) methods have shown promise at effectively controlling ego behavior. However, these methods can struggle in scarce data regimes like those encountered in safety-critical situations. Therefore, the most effective learning method for ego planning remains an unsolved problem.

In this paper, we describe a framework enabling the first successful application and deployment of online safe RL for ego planning in a self-driving environment. When leveraging online RL methods, care needs to be exercised in the environment, action space, and reward design in order to elicit the desired behavior from the resulting policy. In settings like self-driving effectively modeling the environment’s complex transition dynamics and defining complex reward shaping are commonly seen as impediments to online RL; however, we demonstrate results with simple transition dynamics and reward design which can be transferred to the real world.

---

\* All work related to this paper performed while employed by Nuro, Inc.

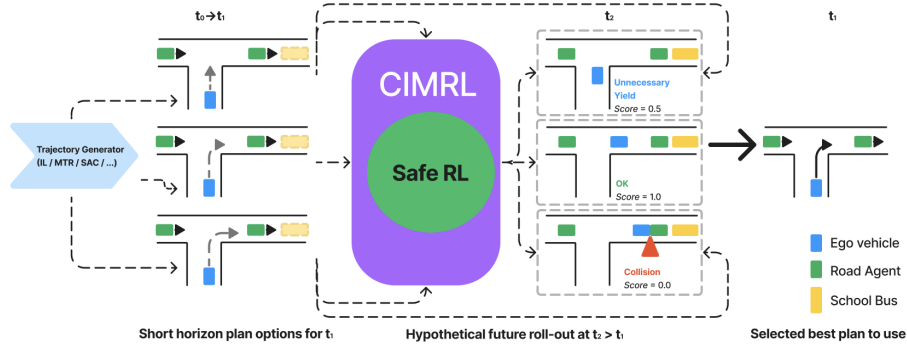


Figure 1: An overview of our approach: CIMRL adopts multiple plan proposals (can be even from different trajectory generators) and other road agent predictions, evaluates them in a closed loop manner for a longer horizon and selects the one that is safe with the maximal score. In the figure, the upper plan is too conservative, while the lower plan is too aggressive (and eventually leads to a future collision), and they both have low scores; the safe and non-conservative plan is chosen as having the highest score.

In the driving domain, it is common to represent action spaces for ego planning as trajectories learned via imitation. While these methods can perform well in open loop, they are known to be susceptible to drift in closed-loop outside of the expert data support. Additionally, these methods can focus on the average case of driving while performing sub-optimally in the long tail of challenging situations.

We address these issues by first, proposing that RL-based methods can be applied to enable better performance in closed loop by learning from states outside the narrow support of expert datasets. One naive method to train RL-based policies is to model the action space as only the immediate action for the next invocation. While appealing in its simplicity, we demonstrate that this choice is suboptimal. We propose to leverage state-of-the-art trajectory prediction models as imitative motion priors and learn a discrete policy to select amongst these quality candidates. By leveraging this method of discretization, we can narrow the exploration problem, ensure human-like policies, and allows for the incorporation of domain knowledge in generating feasible and traffic-rule compliant backup plans. The overview of this combined method is shown in Fig. 1.

Second, given the critical nature of safety concerns, we incorporate explicit risk severity modeling within the context of safe-RL [7]. To address the optimization challenge of balancing reward maximization and risk minimization, we adopt a strategy similar to Recovery RL [7], training two separate policies — one focused on maximizing task reward and the other on minimizing risk severity. Acknowledging the continuous nature of driving and the scarcity of risk events, we employ the Tree Backup [8] algorithm to aid in effectively estimating the task and risk Q value. We then leverage the combined policy, crafted with the assistance of risk estimation, for the final control of the SDC.

The rest of this document is organized as follows: In Section 2 we briefly overview the related work. In Section 3 we describe our approach and the corresponding architecture in the context of the Recovery RL framework. In Section 4 we describe our experimental setup and present the main results. Finally, in Section 5 we conclude and present a few future research directions.

## 2 Related Work

There has been a vast body of work concerning safety in Reinforcement Learning. [9, 10] study this problem by imposing (safety) constraints on expected return. There has been also a large body of work based on measurements of risk [11, 12]. Our work is closely related to [7] which proposes a framework where an agent learns to optimize the task policy while utilizing a (learned) recovery policy that guides the agent back to a safe state when it violates the safety constraints defined in the problem. This hybrid policy aims to ensure that the agent can operate safely within an environment,

effectively mitigating risks and improving the robustness of RL applications in real-world scenarios. In contrast to this work, our approach is not generative in terms of actions; instead, we optimize over a predefined set of motion proposals generated by a previously learned motion generator, such as behavior cloning (BC) policies. These pre-generated motions are generally more likely to remain within safety zones and achieve higher task return while ensuring safer policy exploration in the task space.

Our core RL algorithms are based on the Soft Actor-Critic (SAC) [13] algorithm. More specifically, since we optimize over a finite set of motion proposals we adopted SAC for discrete action settings [14].

A vast body of work in robotics motion planning has focused on a similar trajectory selection problem, where a library of trajectories is generated offline, selected, and composed during runtime. By discretizing the large action space into a finite set of trajectory primitives, these methods can achieve reasonable performance while maintaining an acceptable runtime [15, 16, 17]. Recent methods in this line of work augment trajectory primitives with “funnels” [18, 19, 20], where each funnel is associated with a feedback controller, and the funnel size represents motion uncertainty. They ensure the safety of the robotic system by selecting the funnels (and the associated controllers) with the smallest cost while accounting for uncertainties in motion [21]. Similar techniques use Hamilton-Jacobi-Bellman (HJB) Reachability analysis [22, 23] to precompute a safe set of trajectory parameters offline and select the best trajectory from the set online. While funnel-based motion primitives offer analytical safety guarantees concerning the misalignment between the physics model used for planning and the real world, they do not address uncertainties in other agents’ decisions. In theory, these uncertainties could be embedded into funnel-based primitives; however, identifying decision uncertainty is highly challenging, unlike system identification for physical systems. In contrast, our method trains a closed-loop safety critic using model-free RL by simulating many real-world driving scenarios, bypassing the necessity of explicitly identifying such an uncertainty model.

Our work is also related to learning and planning in hierarchical reinforcement learning [24, 25, 26, 27], specifically within the framework of options [24]. We can view the task and recovery policies as two separate options where we essentially learn the policies and the termination conditions for each. The high-level policy is a fixed policy that switches between these two options depending on the safety criteria and regions.

[28] proposes an approach (BC-SAC) that addresses the limitations of pure imitation learning (IL) by integrating it with reinforcement learning (RL). The hybrid approach combines the strengths of IL and RL, allowing the system to learn from both expert demonstrations and its own experiences, thereby improving driving behavior realism which emerges from IL; and robustness and safety using the closed loop feedback control in RL, in diverse driving scenarios. Our approach differs from this work as follows: (1) BC-SAC directly optimizes a joint IL+RL objective by combining the (offline) expert data likelihood augmented by a (online) reward optimization within an RL framework resulting in a policy defined over primitive motion actions. In contrast, our approach decouples IL and RL, and performs motion planning using the motions generated by a previously learned IL component as the temporally extended actions in a hierarchical RL framework; (2) BC-SAC does not explicitly guarantee multi-criteria safety concerns which are very important in SDC. In contrast, we utilize recovery RL within a safe RL framework to establish safety guarantees in this domain.

### 3 Combining Imitation and Reinforcement Learning (CIMRL)

This section presents a comprehensive overview of our CIMRL system, including the algorithm, model architecture, and distributed training system.

### 3.1 Algorithm

The CIMRL system builds on top of the Recovery-RL [7] which prioritizes the safety of the resulting policy while also ensuring continual progress along the ego route. We outline the holistic approach below.

#### 3.1.1 Recovery RL

SDC constitutes a multi-objective optimization challenge, which includes the maximization of task rewards, such as progress along the ego route, and the minimization of risk, such as avoiding collisions. These conflicting objectives pose substantial challenges in policy optimization, particularly if there is only a single policy.

Recovery RL [7] is a specific constrained safe RL algorithm designed to train two separate policies concurrently, allowing for the effective handling of conflicting objectives. It includes a typical task policy focused on maximizing a task critic alongside a recovery policy aiming at minimizing a separate risk critic that estimates constraint violations. Specifically, it has the following additional objectives:

$$L_{risk} = \|Q_{risk}(s, a) - (r_{risk}(s, a) + \gamma_{risk} \cdot V_{risk}(s'))\|^2$$

$$J_{recovery} = \mathbb{E}_{a \sim \pi_{recovery}} [Q_{risk}(s, a)]$$

where  $V_{risk}(s')$  refers to the expected future risk severity for the next state  $s'$  under the recovery policy  $\pi_{recovery}$  and can be estimated by any applicable RL algorithm. Furthermore, these objectives can be combined with any RL algorithm for learning the task policy which is trained to maximize the task rewards provided by the environment.

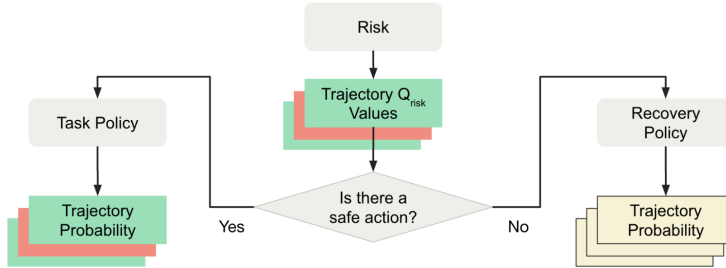


Figure 2: We use the  $Q_{risk}$  estimation to determine the presence of safe actions based on a risk threshold. If such actions exist, we rely on the task policy  $\pi_{task}$  to select exclusively from the safe actions. However, should there be no safe actions available, we fall back to using the recovery policy  $\pi_{recovery}$  to select from all valid actions.

#### 3.1.2 Tree Backup Target

Although Recovery RL was originally formulated for a continuous action space, we have adopted its principles for application within a discrete action space. In CIMRL, we use an actor-critic [13] architecture combined with Tree-Backup [8], an off-policy N-step method for estimating the expected future task and risk state-action value functions. In practice, we designate dense rewards, such as progress, as task rewards, while sparse failure events, such as collisions, are treated as risk rewards. For these sparse risk rewards, a binary flag  $\sigma$  is used to indicate the presence of a risk event. Additionally, we define a scalar value,  $r_{risk}$ , as a measure to reflect the severity associated with the risk event. We train the recovery policy  $\pi_{recovery}$  to minimize the risk severity.

Given that driving is an infinite horizon task, the bootstrapped estimation of the task and risk Q value for the terminal states of the episodes is used to compute the tree backup target. Additionally, in line with Equation IV.1 discussed in Recovery RL [7], we disregarded the discounted future risk severity succeeding the initial risk failure event. Specifically, the target task and risk Q value per timestep  $t$

are calculated as follows assuming discount factor  $\gamma_{task}$  and  $\gamma_{risk}$ :

$$Q_{task}^{target}(s_t, a_t) = \begin{cases} Q_{task}(s_t, a_t), & \text{if } s_t \text{ is terminal} \\ r_{task}(s_t, a_t) + \gamma_{task} \cdot V_{task}(s_{t+1}), & \text{otherwise} \end{cases}$$

$$Q_{risk}^{target}(s_t, a_t) = \begin{cases} Q_{risk}(s_t, a_t), & \text{if } s_t \text{ is terminal} \\ \delta_t \cdot r_{risk}(s_t, a_t) + (1 - \delta_t) \cdot \gamma_{risk} \cdot V_{risk}(s_{t+1}), & \text{otherwise} \end{cases}$$

where  $Q_{task}^{target}$  and  $Q_{risk}^{target}$  are used to update the task and risk critic, employing an  $L_2$  loss as follows:

$$L_{task} = \sum \|Q_{task}(s_t, a_t) - Q_{task}^{target}(s_t, a_t)\|^2$$

$$L_{risk} = \sum \|Q_{risk}(s_t, a_t) - Q_{risk}^{target}(s_t, a_t)\|^2 \quad (1)$$

### 3.1.3 Combined Policy

We employ a hierarchical approach as illustrated in Figure 2 to combine the task policy  $\pi_{task}$  and recovery policy  $\pi_{recov}$  using  $Q_{risk}$ , denoted as  $\pi_{comb}$ . First, actions are filtered using  $Q_{risk}$  based on some hyperparameter risk threshold  $\theta$ , generating a set of safe actions referred to as  $\{A_{safe}\}$ . If this set is not empty, the action selection defaults to  $\pi_{task}$ , focused solely on the remaining available safe actions. However, if all valid actions are deemed unsafe according to  $Q_{risk}$ , the system falls back to relying on  $\pi_{recov}$  to select an action that minimizes the risk from all valid actions.

During inference time, action is selected based on the highest probability as per  $\pi_{comb}$ . During training time, we sample actions based on  $\pi_{comb}$ , supplemented by an exploration strategy like epsilon-greedy or Boltzmann temperature. We also use  $\pi_{comb}$  to compute the task and risk state value per timestep  $t$  as follows:

$$V_{task}(s_t) = p_{\pi_{comb}}(s_t, a_t) \cdot Q_{task}^{target}(s_t, a_t) + \sum_{a' \neq a} p_{\pi_{comb}}(s_t, a') \cdot Q_{task}(s_t, a') \quad (2)$$

$$V_{risk}(s_t) = p_{\pi_{comb}}(s_t, a_t) \cdot Q_{risk}^{target}(s_t, a_t) + \sum_{a' \neq a} p_{\pi_{comb}}(s_t, a') \cdot Q_{risk}(s_t, a') \quad (3)$$

where  $a_t$  denotes the action selected at timestamp  $t$  while  $p_{\pi_{comb}}(s_t, a_t)$  is the probability of executing action  $a_t$  at state  $s_t$  as per  $\pi_{comb}$ . The tree backup target  $Q_{*}^{target}(s_t, a_t)$  is computed as per Eq. 1, and  $Q_{*}(s_t, a_t)$  refers to the estimation of the critic network for the task and risk  $Q$  values. Additionally, we assume the probability of invalid actions, such as unsafe and invalid ones, is masked as 0 during the construction of  $\pi_{comb}$ .

### 3.1.4 Suppressed Task Value

Oftentimes, constrained safe RL algorithms can result in sharp discontinuities in the policy, particularly near the boundaries of constraint violations. To minimize the potential for sharp changes in the policy near safety-critical states, we adopt a strategy similar to [29] to adaptively suppress the task  $Q$  value using the risk  $Q$  value as follows:

$$Q_{supp\_task}(s, a) = \frac{Q_{task}(s, a)}{f(Q_{risk}(s, a))}$$

where  $f(\cdot)$  is a (partition) function of  $Q_{risk}(s, a)$  (e.g., an exponential function such as  $\exp(\cdot)$ ). The task policy aims to maximize this suppressed task  $Q$  value  $Q_{supp\_task}(s, a)$ . This facilitates a smooth interpolation between the conflicting objectives of maximizing task reward while minimizing risk severity. It also modulates the sensitivity to the applied risk threshold  $\theta$  in the combined policy as described in Section 3.1.3, especially in the nearby vicinity of safety-critical states. In practical implementation, we've found it beneficial to suppress  $Q_{task}(s, a)$  only when  $Q_{risk}(s, a)$  exceeds a certain threshold. Moreover, applying a step function  $\lfloor \frac{Q_{risk}(s, a)}{\rho} \rfloor \times \rho$  for some step size  $\rho$  makes the suppressed objective less sensitive to the inherent noise in the  $Q_{risk}(s, a)$  calculation.

### 3.1.5 Policy Loss

In practical applications, we might encounter multiple task rewards and risks. In such cases, we compute a weighted sum of these to obtain a utility measure. In particular, we can compute the task and risk utility as follows:

$$\psi_{task}(s, a) = \sum_i w_i \cdot Q_{supp\_task}^i(s, a)$$

$$\psi_{risk}(s, a) = \sum_j w_j \cdot Q_{risk}^j(s, a)$$

Where  $\omega_i$  and  $\omega_j$  are the hyperparameters that determine the weight assigned to each individual task and risk reward. Given the  $\psi_{task}$  and  $\psi_{risk}$ , we compute the KL-divergence to optimize for the task and recovery policy network.

$$J_{task} = D_{KL}(\pi_{task}(a) \parallel \text{softmax}(\psi_{task}(s, a)))$$

$$J_{recov} = D_{KL}(\pi_{recov}(a) \parallel \text{softmax}(-\psi_{risk}(s, a)))$$

It’s important to note that the recovery policy is trained to minimize risk that is achieved by taking the negative of the risk utility,  $-\psi_{risk}(s, a)$ . One can also experiment with different ratios for the policy entropy loss component in the KL loss to balance between exploration and exploitation.

## 3.2 Model Architecture

The CIMRL model, as illustrated in Figure 3, is based on an actor-critic architecture where there is a shared state encoder backbone with separate heads to predict the task and risk critic, as well as the task and recovery policy.

### 3.2.1 Encoder

**State Encoder:** The choice of the encoder is left to the user and is not specific to our framework. However, in general, a commonly used Transformer architecture [30] could be leveraged to encode track history and map for state embedding at each timestamp. We freeze this part of the state encoder during training.

**Action Encoder:** Most prior work explores RL with a fixed action space (e.g. a globally consistent  $\leftarrow\uparrow\downarrow\rightarrow$  action space in Atari games). In CIMRL, however, we consider the case of a state-dependent action space where the possible actions at every state are produced by an auxiliary system potentially consisting of a combination of an ML trajectory generator and/or a classical planner trajectory generator. Our method is entirely agnostic to the method of producing these trajectories. The model takes as input a variably sized set of 10-second motion plans and projects them into an embedding space using MLPs which is then concatenated with the aforementioned state embedding.

### 3.2.2 Decoder

With the aforementioned state embedding and action embedding, as shown in Figure 3, we concatenate them and use them to predict different outputs as described in detail as follows. We use episodic episodes (e.g. 30s scene) for learning each of the decoder networks.

**Task and Risk Critic Networks:** We build two critic networks, a task critic  $Q_{task}$  and a risk critic  $Q_{risk}$ . Both of these networks are implemented with MLPs on top of the concatenated state and action embeddings. We output a single scalar for each task and risk reward stream associated with each input motion plan.

**Task and Recovery Policy Networks:** We build two policies networks,  $\pi_{risk}$  and  $\pi_{task}$ . Each of these networks is also modeled with MLPs. We output a policy probability for each valid action for each of the policy networks.

**Initialization:** Training an RL model is challenging because the task and risk target are usually computed from a bootstrapped task and risk Q value prediction. Unless we have a pretrained model

from some IL or Offline RL algorithm, the initial policy and critic estimation is usually random and can sometimes lead to very wrong predictions and Diverge the training process. However, in practical problems, each of the task and risk targets has physical meaning. For example, if we know the speed limit for the AD, we can know the maximum progress reward per simulation step and we know the progress task target’s prediction bound using  $\frac{\delta^*}{1-\gamma}$  where  $\delta^*$  denotes the maximum progress and  $\gamma$  is a discounting factor. As for risk, if we are minimizing risk severity, we can safely assume and compute the risk severity as a non-negative value, and we can apply a softplus function  $\log(1 + \exp(x))$  to the raw network’s output. In practice, we found that this careful initialization for the task and risk Q value prediction layer can enable us to train the RL model from scratch and have a stable training process.

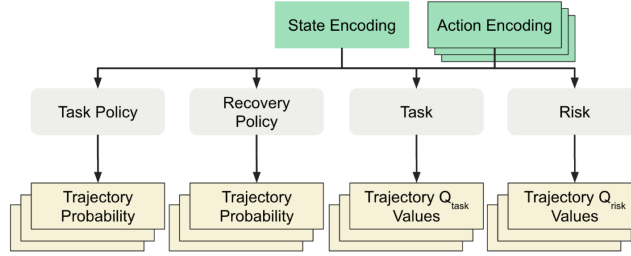


Figure 3: The CIMRL model encodes the state and actions separately and concatenates them to predict value and risk and estimate policy and recovery policy.

## 4 Experiments

The goal of the experimental evaluation is to demonstrate that the successful application of RL on discrete action spaces can outperform baselines relying on imitation and continuous action spaces alone. We compare our method to baselines based on common state-of-the-art methods for the driving domain and provide comparisons on both open-source and proprietary environments to demonstrate the generalizability of our method.

### 4.1 Waymax

The Waymax simulator [31] is a differentiable driving simulator built on top of the standard Waymo Open Motion Dataset and covers a wide range of scenarios ranging in difficulty taken from real-world data. Waymax provides several distinct metrics for evaluation namely: Average Displacement Error (ADE) from the logged ego behavior, Offroad Rate which measures the tendency for the ego to drive off the context map, and Collision Rate. We use an action repeat of 5 in order to both train and evaluate each method which results in a control frequency of 2hz. Since the trajectories output by the MTR model are non-smooth, they produce a noisy yaw signal. We smooth the noise in yaw by applying a low pass filter on the computed yaw before executing the action. In Table 1 we compare the CIMRL with the naive application of MTR as a trajectory generator. Our method strongly outperforms the cloning baseline represented by MTR across ADE as well as collision violations while remaining competitive in offroad violations.

The results show overall that CIMRL can augment and improve upon the closed-loop behavior of an open-loop policy. However, the rate of violations remains high and can be explained by the specific architecture of the MTR model. In closed loop, it is common to accumulate drift over time, and in the case of MTR, the initial goal waypoints are rotated into the ego frame. Error in yaw over time will then lead to offroad goals due to this rotation making it challenging for any policy to recover. This result highlights the differences between open and closed loop benchmarks and suggests that open loop performance might not correlate well with closed loop behavior.



## 4.2 Internal Data

We train our method on hundreds of thousands of scenes from both real onroad data as well as synthetic leveraging trajectories from both a learned model as well as heuristically generated backup plans. Our evaluation dataset consists of 30k scenes covering a wide range of ODD as well as interaction types. These scenes are mined in order to contain challenging scenes for both open loop prediction models as well as capturing long-tail interactions. In Table 2 we compare the naive behavior Cloning (BC) implementation with the CIMRL on top of either only BC trajectories or BC trajectories combined with the heuristic planner proposals.

Table 1: Performance Comparison of Different Methods (Waymax)

Method	Log ADE (m) ↓	Collision Violation (%) ↓	Offroad Violation (%) ↓
MTR (highest prob)	29.93	41.29	14.22
MTR (sample)	30.78	43.28	15.39
CIMRL + Safe RL (Ours)	1.62	16.76	21.65

Table 2: Performance Comparison of Different Methods (In-house)

Method	Collision Violation (%) ↓	Stuck (%) ↓
BC	100.00	100.00
CIMRL (BC)	82.22	54.54
CIMRL (BC+Heuristics)	87.64	16.98

## 5 Conclusions and Future Directions

In this work, we presented a safe reinforcement learning (RL) framework for motion planning in self-driving cars which can be built on top of an imitation learning trajectory generator — and generally speaking, can use any trajectory generator source (e.g., heuristic planners, geometric-based samplers, etc.). Our approach reduces the complexity of the action space to a narrow subset of top motions generated by state-of-the-art motion generators and employs reinforcement learning to select a long-horizon optimization objective. Furthermore, we proposed embedding this framework within a safe RL super-set to incorporate explicit risk severity modeling, which is crucial in any self-driving car algorithm. One interesting future direction would be to use the closed loop feedback and further refine the fixed motions generated by the motion generator component.

**Acknowledgements:** We would like to thank the many people who contributed to this work during design, development, and writing. Specifically we would like to thank Ury Zhilinsky for his technical leadership and support. Zixun Zhang, Jinrui Huang, and Ethan Tang for their support in developing the infrastructure to support development. Jin Ge for her insight. Kai Ang for his early contributions.

## References

- [1] Z. Li, W. Wang, H. Li, E. Xie, C. Sima, T. Lu, Q. Yu, and J. Dai. Bevformer: Learning bird’s-eye-view representation from multi-camera images via spatiotemporal transformers, 2022.
- [2] C. R. Qi, W. Liu, C. Wu, H. Su, and L. J. Guibas. Frustum pointnets for 3d object detection from RGB-D data. *CoRR*, abs/1711.08488, 2017. URL <http://arxiv.org/abs/1711.08488>.
- [3] Y. Zhou and O. Tuzel. Voxelnet: End-to-end learning for point cloud based 3d object detection. *CoRR*, abs/1711.06396, 2017. URL <http://arxiv.org/abs/1711.06396>.



- [4] Y. Chai, B. Sapp, M. Bansal, and D. Anguelov. Multipath: Multiple probabilistic anchor trajectory hypotheses for behavior prediction. *CoRR*, abs/1910.05449, 2019. URL <http://arxiv.org/abs/1910.05449>.
- [5] N. Nayakanti, R. Al-Rfou, A. Zhou, K. Goel, K. S. Refaat, and B. Sapp. Wayformer: Motion forecasting via simple and efficient attention networks, 2022.
- [6] H. Zhao, J. Gao, T. Lan, C. Sun, B. Sapp, B. Varadarajan, Y. Shen, Y. Shen, Y. Chai, C. Schmid, C. Li, and D. Anguelov. TNT: target-driven trajectory prediction. *CoRR*, abs/2008.08294, 2020. URL <https://arxiv.org/abs/2008.08294>.
- [7] B. Thananjeyan, A. Balakrishna, S. Nair, M. Luo, K. Srinivasan, M. Hwang, J. E. Gonzalez, J. Ibarz, C. Finn, and K. Goldberg. Recovery RL: safe reinforcement learning with learned recovery zones. *CoRR*, abs/2010.15920, 2020. URL <https://arxiv.org/abs/2010.15920>.
- [8] K. D. Asis, F. Hernandez-Garcia, Z. Holland, and R. S. Sutton. Multi-step reinforcement learning: A unifying algorithm. *ArXiv*, abs/1703.01327, 2017. URL <https://api.semanticscholar.org/CorpusID:16544526>.
- [9] J. Achiam, D. Held, A. Tamar, and P. Abbeel. Constrained policy optimization. *CoRR*, abs/1705.10528, 2017. URL <http://arxiv.org/abs/1705.10528>.
- [10] C. Tessler, D. J. Mankowitz, and S. Mannor. Reward constrained policy optimization. *CoRR*, abs/1805.11074, 2018. URL <http://arxiv.org/abs/1805.11074>.
- [11] A. Tamar, Y. Chow, M. Ghavamzadeh, and S. Mannor. Policy gradient for coherent risk measures. In C. Cortes, N. Lawrence, D. Lee, M. Sugiyama, and R. Garnett, editors, *Advances in Neural Information Processing Systems*, volume 28. Curran Associates, Inc., 2015. URL [https://proceedings.neurips.cc/paper\\_files/paper/2015/file/024d7f84fff11dd7e8d9c510137a2381-Paper.pdf](https://proceedings.neurips.cc/paper_files/paper/2015/file/024d7f84fff11dd7e8d9c510137a2381-Paper.pdf).
- [12] I. Greenberg, Y. Chow, M. Ghavamzadeh, and S. Mannor. Efficient risk-averse reinforcement learning. In A. H. Oh, A. Agarwal, D. Belgrave, and K. Cho, editors, *Advances in Neural Information Processing Systems*, 2022. URL <https://openreview.net/forum?id=LdAxczs3m0>.
- [13] T. Haarnoja, A. Zhou, K. Hartikainen, G. Tucker, S. Ha, J. Tan, V. Kumar, H. Zhu, A. Gupta, P. Abbeel, and S. Levine. Soft actor-critic algorithms and applications. *CoRR*, abs/1812.05905, 2018. URL <http://arxiv.org/abs/1812.05905>.
- [14] P. Christodoulou. Soft actor-critic for discrete action settings. *CoRR*, abs/1910.07207, 2019. URL <http://arxiv.org/abs/1910.07207>.
- [15] D. Fox, W. Burgard, and S. Thrun. The dynamic window approach to collision avoidance. *IEEE Robotics & Automation Magazine*, 4(1):23–33, 1997.
- [16] M. Pivtoraiko, R. A. Knepper, and A. Kelly. Differentially constrained mobile robot motion planning in state lattices. *Journal of Field Robotics*, 26(3):308–333, 2009.
- [17] D. Dey, T. Liu, B. Sofman, and J. Bagnell. Efficient optimization of control libraries. In *Proceedings of the AAAI Conference on Artificial Intelligence*, volume 26, pages 1983–1989, 2012.
- [18] R. Tedrake, I. R. Manchester, M. Tobenkin, and J. W. Roberts. Lqr-trees: Feedback motion planning via sums-of-squares verification. *The International Journal of Robotics Research*, 29(8):1038–1052, 2010.
- [19] A. Majumdar and R. Tedrake. Funnel libraries for real-time robust feedback motion planning. *The International Journal of Robotics Research*, 36(8):947–982, 2017.

- [20] S. Singh, B. Landry, A. Majumdar, J.-J. Slotine, and M. Pavone. Robust feedback motion planning via contraction theory. *The International Journal of Robotics Research*, 42(9):655–688, 2023.
- [21] R. Alterovitz, T. Siméon, and K. Goldberg. The stochastic motion roadmap: A sampling framework for planning with markov motion uncertainty. 2008.
- [22] S. Kousik, S. Vaskov, F. Bu, M. Johnson-Roberson, and R. Vasudevan. Bridging the gap between safety and real-time performance in receding-horizon trajectory design for mobile robots. *The International Journal of Robotics Research*, 39(12):1419–1469, 2020.
- [23] S. Kousik, S. Vaskov, M. Johnson-Roberson, and R. Vasudevan. Safe trajectory synthesis for autonomous driving in unforeseen environments. In *Dynamic systems and control conference*, volume 58271, page V001T44A005. American Society of Mechanical Engineers, 2017.
- [24] R. S. Sutton, D. Precup, and S. Singh. Between mdps and semi-mdps: A framework for temporal abstraction in reinforcement learning. *Artificial intelligence*, 112(1-2):181–211, 1999.
- [25] R. Parr and S. Russell. Reinforcement learning with hierarchies of machines. In M. Jordan, M. Kearns, and S. Solla, editors, *Advances in Neural Information Processing Systems*, volume 10. MIT Press, 1997. URL [https://proceedings.neurips.cc/paper\\_files/paper/1997/file/5ca3e9b122f61f8f06494c97b1afccf3-Paper.pdf](https://proceedings.neurips.cc/paper_files/paper/1997/file/5ca3e9b122f61f8f06494c97b1afccf3-Paper.pdf).
- [26] T. G. Dietterich. Hierarchical reinforcement learning with the MAXQ value function decomposition. *CoRR*, cs.LG/9905014, 1999. URL <https://arxiv.org/abs/cs/9905014>.
- [27] L. P. Kaelbling and T. Lozano-Pérez. Hierarchical task and motion planning in the now. In *2011 IEEE International Conference on Robotics and Automation*, pages 1470–1477. IEEE, 2011.
- [28] Y. Lu, J. Fu, G. Tucker, X. Pan, E. Bronstein, R. Roelofs, B. Sapp, B. White, A. Faust, S. Whiteson, D. Anguelov, and S. Levine. Imitation is not enough: Robustifying imitation with reinforcement learning for challenging driving scenarios, 2023.
- [29] Z. Zhou, J. Booher, K. Rohanimanesh, W. Liu, A. Petiushko, and A. Garg. Multi-constraint safe rl with objective suppression for safety-critical applications, 2024.
- [30] A. Vaswani, N. Shazeer, N. Parmar, J. Uszkoreit, L. Jones, A. N. Gomez, L. Kaiser, and I. Polosukhin. Attention is all you need. *CoRR*, abs/1706.03762, 2017. URL <http://arxiv.org/abs/1706.03762>.
- [31] C. Gulino, J. Fu, W. Luo, G. Tucker, E. Bronstein, Y. Lu, J. Harb, X. Pan, Y. Wang, X. Chen, J. D. Co-Reyes, R. Agarwal, R. Roelofs, Y. Lu, N. Montali, P. Mouglin, Z. Yang, B. White, A. Faust, R. McAllister, D. Anguelov, and B. Sapp. Waymax: An accelerated, data-driven simulator for large-scale autonomous driving research, 2023.